Journal of Statistical Physics, Vol. 93, Nos. 3/4, 1998

Viscous Fingering Patterns in Ferrofluids

Michael Widom[1] and José A. Miranda[1,2]

Received February 2, 1998

Viscous fingering occurs in the flow of two immiscible, viscous fluids between the plates of a Hele–Shaw cell. Due to pressure gradients or gravity, the initially planar interface separating the two fluids undergoes a Saffman–Taylor instability and develops fingerlike structures. When one of the fluids is a ferrofluid and a perpendicular magnetic field is applied, the labyrinthine instability supplements the usual viscous fingering instability, resulting in visually striking, complex patterns. We consider this problem in a rectangular flow geometry using a perturbative mode-coupling analysis. We deduce two general results: viscosity contrast between the fluids drives interface asymmetry, with no contribution from magnetic forces; magnetic repulsion within the ferrofluid generates finger tip-splitting, which is absent in the rectangular geometry for ordinary fluids.

KEY WORDS: Ferrofluid; pattern formation; mode coupling; Saffman–Taylor instability.

1. INTRODUCTION

The Saffman–Taylor problem,[1] in which two immiscible, viscous fluids move in a narrow space between the parallel plates of a Hele–Shaw cell, is a widely studied example of hydrodynamic pattern formation where interfacial instabilities grow and evolve.[2] The initially flat interface separating the two fluids is destabilized by either a pressure gradient advancing the less viscous fluid against the more viscous one, or by gravity coupling to a density difference between the fluids.

Ferrofluids, colloidal suspensions of microscopic permanent magnets, respond paramagnetically to applied fields.[3] Because they are liquids, they flow in response to magnetic forces. Ferrofluids confined within Hele–Shaw cells exhibit interesting interfacial instabilities. One of the most beautiful,

[1] Department of Physics, Carnegie Mellon University, Pittsburgh, Pennsylvania 15213.
[2] Departamento de Fisica, Universidade Federal de Pernambuco, Recife, PE 50670-901, Brazil.

0022-4715/98/1100-0411$15.00/0

the labyrinthine instability, occurs when a magnetic field is applied perpendicular to the Hele–Shaw cell. Elements of magnetized liquid repel each other, creating highly branched, intricately fingered structures.

Recent experiments[4] examine the Saffman–Taylor instability, when one of the two fluids is a ferrofluid, in the presence of a perpendicular magnetic field. The resulting interfacial patterns, in a rectangular Hele–Shaw cell, are an intriguing superposition of familiar forms from ordinary viscous fingering and labyrinthine patterns. Two immediately striking features of the patterns: The pattern of low viscosity fluid penetrating into high viscosity fluid is totally unlike the pattern of high viscosity fluid penetrating into low viscosity fluid; Finger splitting is prevalent, while in general it is completely absent in zero external magnetic field.

We explain these two phenomena within a perturbative approach known as mode-coupling theory. Linear stability analysis explains the instability of an initially flat interface to sinusoidal perturbations known as modes. In the initial, linear stage of pattern formation, modes grow or decay independently of each other. One mode, which we call the "fundamental," grows faster than all others. As these perturbations of the flat interface grow, they evolve through a weakly non-linear stage, in which modes couple with each other, to the strongly nonlinear late stages in which a Fourier decomposition of the interface shape becomes inappropriate.

We carry out our mode-coupling expansion to third order. Linear stability analysis explains neither interfacial symmetry breaking nor finger tip-splitting. At second order, we find the viscosity contrast A (defined as the difference between the two fluid viscosities divided by their sum) breaks the symmetry of the interface by enhancing growth of subharmonic perturbations to the fundamental mode. This mechanism occurs independently of the applied magnetic field. At third order we find a mechanism for finger tip-splitting driven by mutual repulsion of elements of magnetic fluid. In the absence of a magnetic field, finger tips do not split in rectangular geometry Hele–Shaw flow.

2. HYDRODYNAMICS IN A HELE–SHAW CELL

This section begins with a discussion of basic hydrodynamic equations governing the motion of fluids confined within a Hele–Shaw cell, considering ferrofluid in particular. We present Darcy's law in the presence of a perpendicular magnetic field, and we discuss boundary conditions obeyed at the two-fluid interface. Since the basic equations are well established by previous investigators, we simply review the chief assumptions and results. This section concludes by describing our perturbative approach. We introduce a Fourier decomposition of the interface shape and derive coupled,

nonlinear, ordinary differential equations governing the time evolution of Fourier amplitudes.

2.1. Governing Equations

Consider two semi-infinite immiscible viscous fluids, flowing in a narrow gap of thickness b, between two parallel plates (see Fig. 1). Denote the densities and viscosities of the lower and upper fluids, respectively as ρ_1, η_1 and ρ_2, η_2. Between the two fluids there exists a surface tension σ. Inject fluid 1 at constant external flow velocity $\vec{v}_\infty = v_\infty \hat{y}$ at $y = -\infty$ and withdraw fluid 2 at the same velocity at $y = +\infty$. We describe the system in a frame moving with velocity $\vec{v}_\infty$, so that the interface may deform, but it does not displace from $y = 0$ (dashed line in Fig. 1) on the average. During the flow, the interface has a perturbed shape described as $y = \zeta(x, t)$ (solid curve in Fig. 1) over the range $0 \leqslant x \leqslant L$ in the comoving frame.

In order to include the acceleration of gravity $\vec{g}$, we tilt the cell so that the y axis lies at angle β from the vertical direction. To include magnetic forces, we apply a magnetic field $\vec{H}_0$ at right angles to the cell. By assumption, the upper fluid acquires magnetization $\vec{M}$, while the lower fluid is non-magnetic. We consider the limit $L \to \infty$ to simplify calculations of magnetic forces.

Hydrodynamics of ferrofluids differs from the usual Navier–Stokes equations through the inclusion of a term representing magnetic force.[3] Let $\vec{M}$ represent the local magnetization of the ferrofluid, and note that the

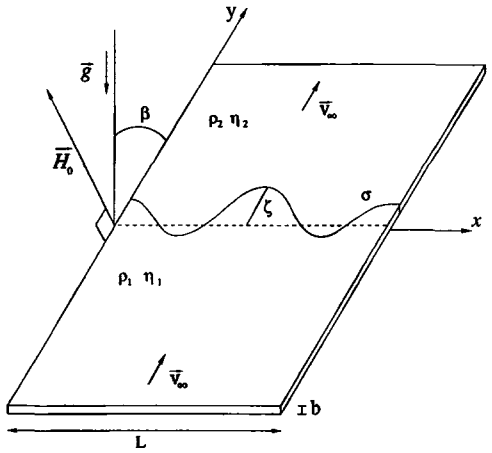

Fig. 1. Schematic configuration of the rectangular flow geometry. The upper fluid is a ferrofluid.

force on $\vec{M}$ depends on the gradient of local magnetic field $\vec{H}$. The local field differs from the applied field by the demagnetizing field of the polarized ferrofluid. Restricting our attention to small velocity flows of viscous fluids, we ignore the inertial terms and write the Navier–Stokes equation for a single fluid

$$-\eta\nabla^2\vec{u} = -\vec{\nabla}p + (\vec{M}\cdot\vec{\nabla})\,\vec{H} + \rho\vec{g} \tag{1}$$

For the two dimensional geometry of a Hele–Shaw cell, the three dimensional flow $\vec{u}$, governed by Eq. (1), may be replaced with an equivalent two-dimensional flow $\vec{v}$ by averaging over the z direction perpendicular to the plane of the Hele–Shaw cell. Imposing no-slip boundary conditions, a parabolic velocity profile and assuming constant magnetization parallel to $\vec{H}_0$, one derives Darcy's law for ferrofluids in a Hele–Shaw cell,[5,6]

$$\eta\vec{v} = -\frac{b^2}{12}\left\{\vec{\nabla}p - \frac{2M}{b}\vec{\nabla}\varphi - \rho(\vec{g}\cdot\hat{y})\,\hat{y}\right\} \tag{2}$$

The magnetic scalar potential φ is evaluated on the top plate of the cell. The velocity depends on a linear combination of gradients of p and φ, so we may think of the magnetic scalar potential as part of an effective pressure. Equation (2) describes nonmagnetic fluids by simply dropping the terms involving magnetization.

It is convenient to rewrite Eq. (2) in terms of velocity potentials because the velocity field $\vec{v}$ is irrotational. Since we are interested in perturbations of the velocity field around a steady flow, we write $\vec{v} = \vec{v}_\infty - \vec{\nabla}\phi$, where ϕ defines the velocity potential. Both sides of Eq. (2) are recognized as gradients of scalar fields. Integrating both sides of Eq. (2) yields

$$\eta\phi = \frac{b^2}{12}\left\{p - \frac{2M}{b}\varphi + \rho g y\cos\beta\right\} + \eta v_\infty y \tag{3}$$

after dropping an arbitrary constant of integration.

Subtract Eq. (3) for one fluid from the same equation for the other fluid, then divide by the sum of the two fluids' viscosities. This yields an equation for the discontinuity of velocity potentials valid at the two-fluid interface

$$A\left(\frac{\phi_2+\phi_1}{2}\right) + \left(\frac{\phi_2-\phi_1}{2}\right) = \frac{b^2}{12(\eta_1+\eta_2)}\left((p_2-p_1) - \frac{2M}{b}\varphi_s\right) + Uy \tag{4}$$

The viscosity contrast

$$A = \frac{\eta_2 - \eta_1}{\eta_2 + \eta_1} \tag{5}$$

will play a key role in interfacial symmetry breaking. U is a characteristic velocity associated with driving forces,

$$U = \frac{b^2(\rho_2 - \rho_1)\, g \cos\beta}{12(\eta_1 + \eta_2)} + Av_\infty \tag{6}$$

The pressure jump across the interface, $p_1 - p_2$ depends on κ, the interfacial curvature in the plane of the Hele–Shaw cell. In general this relationship depends upon the discontinuity of the viscous stress tensor. Under the assumption of low capillary number flow we neglect that dependence and write simply

$$p_2 - p_1 = \sigma\kappa \tag{7}$$

We substitute the pressure jump boundary condition (7) into equation (14) and also introduce dimensionless variables, scaling all lengths by the gap size b, and all velocities by the characteristic velocity $\sigma/12(\eta_1 + \eta_2)$. The final equation of motion reads

$$A(\phi_2|_{y=\zeta} + \phi_1|_{y=\zeta}) + (\phi_2|_{y=\zeta} - \phi_1|_{y=\zeta}) = 2[\,Uy + \kappa - N_B \mathscr{I}\,]|_{y=\zeta} \tag{8}$$

N_B is the dimensionless magnetic Bond number

$$N_B = \frac{2M^2 b}{\sigma} \tag{9}$$

and the integral

$$\mathscr{I} = \int_{-\infty}^{\infty} dx' \int_{\zeta(x')}^{\infty} dy' \left[\frac{1}{\sqrt{(x-x')^2 + (y-y')^2}} - \frac{1}{\sqrt{(x-x')^2 + (y-y')^2 + 1}} \right] \tag{10}$$

is proportional to the magnetic scalar potential. Equation (8) governs the flow for a given interface shape ζ.

2.2. Mode-Coupling Analysis

We begin by representing the net perturbation $\zeta(x, t)$ in the form of a Fourier series

$$\zeta(x, t) = \sum_k \zeta_k(t) \exp(ikx) \tag{11}$$

where $\zeta_k(t)$ denotes the complex Fourier mode amplitudes. Expansion (11) includes a discrete (rather than continuous) set of modes k because we focus on the interaction of three particular modes in the subsequent discussion. The $k=0$ mode vanishes since we are in a comoving frame. The wavevectors are constrained to lie on the x axis, but can be either positive or negative.

Now define Fourier expansions for the velocity potentials ϕ_i, which must obey Laplace's equation $\nabla^2\phi_i = 0$, the boundary conditions at $y \to \pm\infty$, and include the discrete modes k entering the Fourier series (11). The general velocity potentials obeying these requirements are

$$\phi_1 = \sum_{k \neq 0} \phi_{1k}(t) \exp(|k|\ y) \exp(ikx) \tag{12}$$

and

$$\phi_2 = \sum_{k \neq 0} \phi_{2k}(t) \exp(-|k|\ y) \exp(ikx) \tag{13}$$

In order to substitute expansions (12) and (13) into the equation of motion (8), we need to evaluate them at the perturbed interface. For example, expand the lower fluid velocity potential $\phi_1|_{y=\zeta}$, evaluated at the perturbed interface, to third order in ζ. Its Fourier transform is

$$\hat{\phi}_1(k) = \phi_{1k}(t) + \sum_{k'} |k'|\, \phi_{1k'}(t)\, \zeta_{k-k'} + \tfrac{1}{2} \sum_{k', q} (k')^2\, \phi_{1k'}(t)\, \zeta_q \zeta_{k-k'-q}. \tag{14}$$

A similar expression for $\phi_2|_{y=\zeta}$ can be easily obtained. These results define the Fourier transform of the left-hand-side of Eq. (8).

Now we must evaulate the Fourier transform of the right-hand-side of Eq. (8). The curvature in the $x-y$ plane is[7]

$$\kappa = \left(\frac{\partial^2\zeta}{\partial x^2}\right)\left[1 + \left(\frac{\partial\zeta}{\partial x}\right)^2\right]^{-3/2} \tag{15}$$

We expand this up to third order in ζ and Fourier transform,

$$\hat{\kappa}(k) = -k^2\zeta_k - \tfrac{3}{2}\sum_{k',\, q\neq 0} (k')^2\, q[k-k'-q]\, \zeta_{k'}\zeta_q\zeta_{k-k'-q} \tag{16}$$

The expansion to third order in powers of ζ, of the integral (10) related to magnetic scalar potential, is

$$\mathscr{I}(x) = \int_{-\infty}^{\infty} \left[\frac{1}{[(x-x')^2]^{1/2}} - \frac{1}{[(x-x')^2+1]^{1/2}}\right] [\zeta(x')-\zeta(x)]\, dx'$$
$$-\frac{1}{6}\int_{-\infty}^{\infty} \left[\frac{1}{[(x-x')^2]^{3/2}} - \frac{1}{[(x-x')^2+1]^{3/2}}\right] [\zeta(x')-\zeta(x)]^3\, dx' \tag{17}$$

When Fourier transformed, the integrals in (17) can be solved in terms of modified Bessel functions[8]

$$K_\nu(k\tau) = \frac{\Gamma(\nu+1/2)}{k^\nu \Gamma(1/2)}(2\tau)^\nu \int_0^\infty \frac{\cos kx}{(x^2+\tau^2)^{\nu+1/2}}\, dx \tag{18}$$

We define the functions

$$J(k) \equiv \log\left(\frac{|k|}{2}\right) + K_0(|k|) + C \tag{19}$$

with C the Euler constant, and

$$T(k) \equiv 3\,|k|\,[\,|k|\,(4\log 2 - 3\log 3) + 2K_1(3\,|k|) - 4K_1(2\,|k|) + 2K_1(|k|) - \tfrac{2}{3}] \tag{20}$$

and write the Fourier transform

$$\hat{\mathscr{I}}(k) = -2J(k)\,\zeta_k + \tfrac{1}{6}\sum_{k',\, q} T(k-k'-q)\,\zeta_{k'}\zeta_q\zeta_{k-k'-q} \tag{21}$$

For nonzero k, $J(k)$ is positive and $T(k)$ is negative. The expansion in powers of ζ can easily be extended to arbitrarily high order. Tsebers[9] presents $\hat{\mathscr{I}}(k)$ up to the fifth order term.

To close Eq. (8) we need additional relations expressing the velocity potentials in terms of the perturbation amplitudes. To find these, consider the kinematic boundary condition relating the interface shape back to the

fluid flow. The condition that the interface move according to the local fluid velocities is written

$$\frac{\partial \zeta}{\partial t} = \left(\frac{\partial \zeta}{\partial x}\frac{\partial \phi_i}{\partial x}\right)_{y=\zeta} - \left(\frac{\partial \phi_i}{\partial y}\right)_{y=\zeta} \tag{22}$$

Expand this to third order in ζ and then Fourier transform. Solving for $\phi_{ik}(t)$ consistently to third order in ζ yields

$$\phi_{1k}(t) = -\frac{\dot{\zeta}_k}{|k|} + \sum_{k'} sgn(kk')\,\dot{\zeta}_{k'}\zeta_{k-k'} - \sum_{k',q}\frac{kq}{|k|}\,sgn(k'q)\,\dot{\zeta}_{k'}\zeta_{q-k'}\zeta_{k-q}$$
$$+ \sum_{k',q}\frac{k'}{|k|}\left(k-q-\frac{k'}{2}\right)\dot{\zeta}_{k'}\zeta_q\zeta_{k-k'-q} \tag{23}$$

and a similar expression for $\phi_{2k}(t)$. The *sgn* function equals ± 1 according to the sign of its argument. The overdot denotes total time derivative.

Substitute this last expression for $\phi_{1k}(t)$ into Eq. (14) for the Fourier transform of $\phi_1|_{y=\zeta}$, and again keep only cubic terms in the perturbation amplitude. Repeat the same procedures for fluid 2. The velocity potentials have now been eliminated from Darcy's law (8), and the differential equation of the interface is

$$\dot{\zeta}_k = \lambda(k)\,\zeta_k + A\,|k| \sum_{k'\neq 0}[1 - sgn(kk')]\,\dot{\zeta}_{k'}\zeta_{k-k'}$$
$$+ \sum_{k',q}|k|\,|q|\,sgn(k'q)[1-sgn(kq)]\,\dot{\zeta}_{k'}\zeta_{q-k'}\zeta_{k-q}$$
$$+ \sum_{k',q}k'\left[k-q-\frac{k'}{2}-\frac{|k'|\,|k|}{2k'}\right]\dot{\zeta}_{k'}\zeta_q\zeta_{k-k'-q}$$
$$- \sum_{k',q}\left[\frac{1}{6}N_B T(k-k'-q) + \frac{3}{2}|k|\,(k')^2\,q[k-k'-q]\right]\zeta_{k'}\zeta_q\zeta_{k-k'-q} \tag{24}$$

Here

$$\lambda(k) = |k|\,[U + 2N_B J(k) - k^2] \tag{25}$$

is the dimensionless linear growth rate multiplying the first order term in ζ. The second term in Eq. (24) is second order in ζ, and the remaining terms constitute the third order contribution.

3. WEAKLY NONLINEAR EVOLUTION

This section analyzes the evolution of an interface under the mode-coupling Eq. (24) derived in Section 2.2. We systematically examine terms in order of their strength at the onset of the instability. Thus, we begin by describing the first order term, which captures the well known linear instability leading to viscous finger growth. Driving forces causing the instability include magnetic repulsion within the ferrofluid. We move on to the second order term, noting the interesting coupling of a fundamental mode and its own subharmonic. This term is responsible for finger competition. Magnetic forces do not contribute to this, or any even order, term. Rather, finger competition depends upon the viscosity contrast A. We conclude our discussion at third order. Here, we show that finger tips may split due to coupling of a fundamental mode with its own harmonic. The process depends upon the presence of magnetic repulsion within the ferrofluid. It does not occur without a magnetic field.

3.1. First Order

First order in the mode-coupling expansion reproduces conventional linear stability analysis. Each mode grows or decays independently of all others, with exponential growth rate $\lambda(k)$ given in Eq. (25). Positive values of $\lambda(k)$ make a mode unstable to growth of an initially small perturbation. Figures 2–4 plot this function for three distinct cases: $U=-1$, $U=0$ and $U=+1$ respectively. For each value of U we graph $\lambda(k)$ for three values of the magnetic Bond number, $N_B=0, 2, 4$.

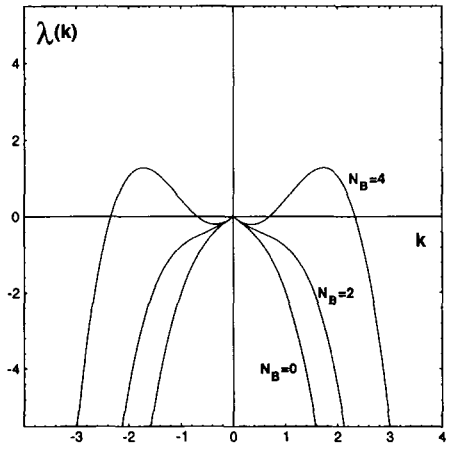

Fig. 2. Plot of $\lambda(k)$ for $U=-1$.

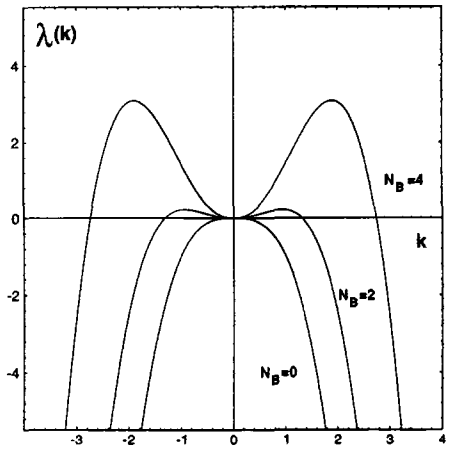

Fig. 3. Plot of $\lambda(k)$ for $U=0$.

In general these plots display a range of wavenumbers over which $\lambda(k)>0$. We define two special wavenumbers: k^*, the wavenumber of the fastest growing mode, maximizes $\lambda(k)$; k_c, the threshold wavenumber beyond which all modes are stable, is the largest wavenumber for which $\lambda(k)$ vanishes. When $U=1$ and $N_B=0$ we have $k_f=1/\sqrt{3}$ and $k_c=1$. The magnetic field is destabilizing. As the magnetic Bond number grows, k^* and k_c shift to the right and modes of higher wavenumber become unstable. Likewise, for any particular mode k, the growth rate $\lambda(k)$ increases, causing perturbations to grow more rapidly.

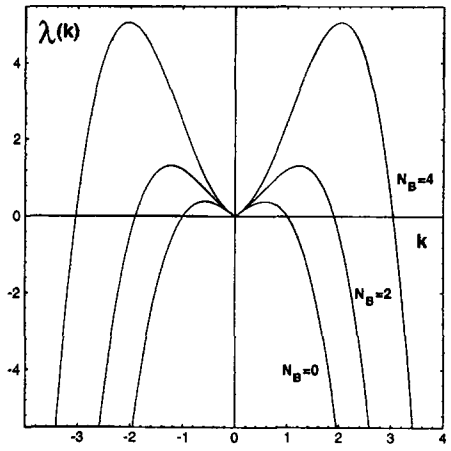

Fig. 4. Plot of $\lambda(k)$ for $U=1$.

To analyze mechanisms of pattern selection, we will focus our attention on the interaction of one large amplitude perturbation, which we call the "fundamental," with small amplitude perturbations of its own harmonic and subharmonic. We take the fundamental wavenumber $k_f = k^*$ of the fastest growing mode. The harmonic mode $k_h = 2k_f$ always lies to the right of the threshold wavenumber k_c, so the harmonic mode is always linearly stable against growth. The subharmonic mode $k_s = k_f/2$ usually lies in the unstable regime. If present in the initial conditions it will grow, but less quickly than the fundamental.

Growth of the fundamental mode creates a sinusoidal oscillation of the initially flat interface, forming fingers of each fluid penetrating into the region previously occupied by the other fluid. The interface is symmetric, with upwards and downwards fingers having identical length and width. Depending upon the phase of the subharmonic relative to the fundamental, either the upwards-pointing fingers, or the downwards pointing fingers may have their length modulated. The subharmonic can break the up-down symmetry of the growing pattern. However, within the linear stability analysis, no unique phase of the subharmonic is favored. Assuming the relative phase is determined by random perturbation of the flat interface, the growing pattern will retain *statistical* up-down symmetry. For any given initial condition, symmetry will be broken, but averaged over all initial conditions, symmetry will remain.

Splitting of fingers is not predicted by linear stability analysis, because the harmonic mode is required to split fingers, and the harmonic mode is linearly stable.

3.2. Second Order

Inspecting the mode coupling Eq. (24), we note that the second order term does not involve magnetic field. We have previously[10] analyzed the role of the second order term in rectangular flow geometry for nonmagnetic fluids. The results are unchanged, so we will simply recall two essential facts: the second order term generates finger competition dependent upon the viscosity contrast A; the second order term does not generate finger tip-splitting. We explain these two points briefly.

Finger competition is linked with the amplitude and phase of the subharmonic mode. Coupling of the fundamental k_f to the growth of its subharmonic k_s accelerates growth of the subharmonic, and selects a preferred phase. The selected phase varies the relative lengths of fingers of the less viscous fluid penetrating into the more viscous fluid. Fingers of more viscous fluid penetrating into the less viscous fluid tend toward equal

lengths. The subharmonic therefore breaks the statistical up-down symmetry of the linear stability theory.

Finger tip-splitting requires the harmonic mode. In the radial flow geometry,[11] second order terms drive growth of the harmonic mode k_h despite its linear stability. These terms are absent due to the rectangular flow geometry. As we explain in the following section, one must examine the third order terms to understand growth of the harmonic.

We conclude this discussion with an explanation for the absence of magnetic field effects at second order. Although the basic equation of motion (2) is written in terms of forces, it is simplest to carry out the discussion in terms of energies. Consider the magnetic energy for a given interface shape $\zeta(x)$. The magnetic energy is unaffected by rotation of the entire experiment (Hele–Shaw cell and magnet) by 180° around the x axis. Because the ferrofluid is paramagnetic, the magnetic energy is invariant under reversing the direction of the applied field. The combination of the two symmetries, rotation of the experiment followed by reversal of the applied field, amounts to reversing the sign of the interfacial displacement $\zeta(x)$. Since the magnetic energy cannot be affected by this change, it must be an even function of $\zeta(x)$. The magnetic force is given by the change in magnetic energy with respect to variation in interfacial shape, so it must be an odd function of $\zeta(x)$.

3.3. Third Order

This section shows how the magnetic field qualitatively alters the mechanism for splitting of finger tips. We first review previous results explaining the general absence of tip splitting in rectangular geometry flow of ordinary fluids.[10] Then we describe a new mechanism for splitting finger tips in the presence of a magnetic field.

We consider the influence of the fundamental and sub-harmonic modes on the growth of the first harmonic. Finger tip-splitting is associated with the magnitude and phase of the harmonic mode $2k_f$. It is convenient for the subsequent discussions to consider sine and cosine modes, rather than the complex modes employed in Eq. (24). Describing the fundamental as a cosine mode with positive amplitude, we only need to examine the subharmonic and harmonic cosine modes to analyze finger competition and tip-splitting. Let a_k denote the amplitude of the cosine mode of wavenumber k.

Earlier papers considered finger tip-splitting for Hele–Shaw flow of nonmagnetic fluids in the radial[11] and rectangular[10] geometries. Of course, the same results hold for ferrofluids in the absence of applied magnetic fields. The principal results are as follows. In the radial geometry,

a term proportional to $a_{k_f}^2$ drives growth of the harmonic with the phase appropriate to split finger tips. In the rectangular geometry, this second order term is missing. Instead, there is a third order driving term proportional to $a_{k_f}a_{k_s}^2$. This term is expected to be too small to split finger tips. There is also a reduction in the effective stability of the harmonic mode for large amplitude of the fundamental, but this effect cannot make the harmonic linearly unstable. Consequently, finger tips do not split under normal circumstances in the rectangular geometry.

Now we investigate the connection between the applied magnetic field and the occurrence of finger tip-splitting observed in Hele–Shaw cell experiments with ferrofluids. For consistency with experimental results[4] we consider the case $U=1$. The equation of motion for the harmonic mode (neglecting terms of order $\mathcal{O}(a_{k_h}^3)$) is

$$\dot{a}_{k_h}=\lambda_{\text{eff}}a_{k_h}-\{\tfrac{3}{8}k_hk_s^2k_f[k_f+2k_s]+N_Bk_h[\tfrac{1}{12}T(k_s)+\tfrac{1}{24}T(k_f)]\}\,a_{k_f}a_{k_s}^2 \tag{26}$$

We incorporate certain third order terms into the effective linear growth rate

$$\lambda_{\text{eff}}=\lambda(k_h)+\left\{\frac{k_f^2k_h}{2}\left[\left(k_f^2+\frac{3}{2}k_h^2\right)-1\right]-N_Bk_h\left[\frac{1}{6}T(k_f)+\frac{1}{12}T(k_h)\right]\right\}a_{k_f}^2$$
$$+\left\{\frac{k_s^2k_h}{2}\left[\left(k_s^2+\frac{3}{2}k_h^2\right)-1\right]-N_Bk_h\left[\frac{1}{6}T(k_s)+\frac{1}{12}T(k_h)\right]\right\}a_{k_s}^2 \tag{27}$$

In Eqs. (26) and (27) some terms are explicitly multiplied by N_B and others are not. We refer to the former as "magnetic" terms, and the latter as "nonmagnetic." The nonmagnetic terms reproduce the known mode coupling equation for nonmagnetic fluids.[10]

Our mechanism for splitting finger tips focuses on λ_{eff}. Initially, this quantity is close to $\lambda(k_h)$, which is strongly negative because the harmonic mode is stable in the linear theory. However, λ_{eff} is increased by the presence of the modes k_f and k_s, because the coefficients multiplying their squared amplitudes are positive. To verify this point, recall that $k_f \geqslant 1/\sqrt{3}$, making the nonmagnetic contribution manifestly positive. Also, the values of $T(k)$ are negative, making the magnetic contribution manifestly positive. Since we consider the case in which a_{k_f} is considerably larger than a_{k_s}, the dominant corrections to the effective growth rate come from the terms multiplying $a_{k_f}^2$. In the following, we concentrate our discussion on those terms.

Nonmagnetic terms make the effective growth rate less negative but cannot make it go positive. The physical reason that these terms do not

make λ_{eff} positive can be understood by considering the contour length of the interface. Introducing the harmonic always increases the contour length, although the larger the amplitude of the fundamental, the smaller the increase upon introducing the harmonic. Multiplying the contour length by the surface tension yields surface energy that favors minimum contour length. Mathematically, the nonmagnetic term of order $a_{k_f}^2$ makes λ_{eff} less negative, but if higher orders in perturbation theory were included it would be evident that a_{k_f} cannot drive λ_{eff} positive without assistance from the magnetic terms.

The terms in λ_{eff} that are multiplied by N_B allow λ_{eff} to eventually go positive, permitting growth of the harmonic. The effective growth rate remains negative up to a threshold value of a_{k_f} for which $\lambda_{\text{eff}} = 0$. When a_{k_f} grows beyond this threshold value, a_{k_h} grows rapidly. The threshold value of a_{k_f} should vary as the inverse square root of the magnetic Bond number, so tip splitting emerges sooner in strong magnetic fields.

The harmonic mode enters spontaneously through the third order driving term proportional to $a_{k_f} a_{k_s}^2$ in Eq. (26). As long as λ_{eff} remains negative, this small driving force should be of little consequence. After λ_{eff} goes positive, however, this term can introduce a harmonic even if none is present in initial conditions. The existence and phase of the spontaneously generated harmonic depends on interplay of the fundamental and the sub-harmonic.

To illustrate the occurrence of finger tip-splitting when an external magnetic field is applied, we consider the interaction of modes k_f and $k_f/2$ with the forced modes $2k_f$ and $3k_f/2$. Mode $3k_f/2$ behaves similarly to the sub-harmonic $k_f/2$ and induces more finger competition. In Fig. 5 we plot

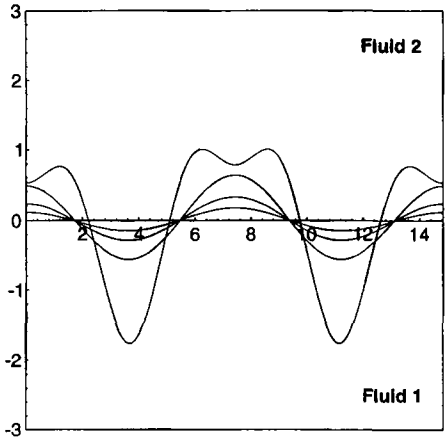

Fig. 5. Plot of an evolving interface with an applied magnetic field.

the interface evolution using the full solution to third order of Eq. (24). We examine the case in which $U=1$, assuming that fluid 2 is a ferrofluid. An external magnetic field is applied ($N_B=1.0$) normal to the cell plates. The initial condition is $a_{k_h}=0.145$ and $a_{k_s}=-1/5\,a_{k_f}$. The harmonic mode is absent initially. Times shown are $t=0$, 1, 2, 3.

The effective harmonic growth rate λ_{eff} starts being strongly negative at $t=0$. It increases with time, goes through zero $t\approx 2.16$, and become positive. This process leads to finger tip-splitting by $t=3$, as shown in Fig. 5. Finger tip-splitting only occurs after the fundamental has grown sufficiently that λ_{eff} goes positive. The selected phase of the harmonic splits the tips of fingers whose length is variable, the less viscous fingers.

4. CONCLUSION

Several features of the patterns formed in Saffman–Taylor experiments[4] with ferrofluids can now be explained. First of all, there is the striking asymmetry of the interface. Since the dense upper fluid is a glycerine-based ferrofluid with high viscosity, and the less dense lower fluid is white spirit, we can understand the initial asymmetry of the interface purely on the basis of the viscosity contrast A, as discussed in Section 3.2. Indeed, with the field turned off the interface is quite asymmetric, with short and wide upwards fingers of the less viscous fluid and long, thin downward fingers of the more viscous fluid. Magnetic field effects can exaggerate an already asymmetric interface, but they cannot break the symmetry by themselves. It would be of considerable interest to perform the experiment with immiscible viscosity-matched fluids.

Next, there is the splitting of finger tips which is not normally observed in rectangular geometry flow. Both upwards and downwards fingers are split, consistent with a positive value of λ_{eff} permitting the growth of harmonics of any phase. The upwards fingers are more strongly split, however, consistent with the phase preferred by the driving force in Eq. (26). Both are predictions of our third order analysis in Section 3.3. It would be of interest to examine the relationship between the onset of tip splitting and the strength of applied magnetic field experimentally.

The above features are explained by our mode coupling theory. Another notable feature of the patterns is the nearly constant width and regular spacing of downward pointing fingers of high viscosity fluid. The constant width is probably the known field-dependent preferred finger width of the labyrinthine instability,[3] proportional to the plate spacing b. Given a directed set of thin fingers, magnetic forces will drive them towards maximal spacing, resulting in a regularly spaced array. These issues lie

beyond the scope of our low order mode coupling approach, but may be amenable to more general forms of weakly nonliner analysis.

ACKNOWLEDGMENTS

We thank Christiane Caroli for suggesting this research topic, and the ferrofluid research group at the University of Paris (Pierre et Marie Curie) for demonstrating the hydrodynamic flows analyzed in this paper. This work was supported in part by the National Science Foundation grant No. DMR-9732567. J.A.M. (CNPq reference number 200204/93-9) would like to thank CNPq (Brazilian Research Council) for financial support. M.W. thanks Leo P. Kadanoff for stimulating discussions on the subject of viscous fingering in 1983 and later.

REFERENCES

1. P. G. Saffman and G. I. Taylor, *Proc. R. Soc. London Ser. A* **245**:312 (1958).
2. For recent reviews on this fascinating subject see K. V. McCloud and J. V. Maher, *Phys. Rep.* **260**:139 (1995); A. A. Sonin, *Rivista del Nuovo Cimento* **14**:1 (1991); P. G. Saffman, *IMA J. Appl. Math.* **46**:137 (1991); D. Bensimon, L. P. Kadanoff, S. Liang, B. I. Shraiman, and C. Tang, *Rev. Mod. Phys.* **58**:977 (1986).
3. R. E. Rosensweig, *Ferrohydrodynamics* (Cambridge University Press, Cambridge, 1985).
4. R. Perzynski *et al.* (unpublished).
5. D. P. Jackson, R. E. Goldstein, and A. O. Cebers, *Phys. Rev. E* **50**:298 (1994).
6. A. O. Cebers, *Magnetohydrodynamics* 17:113 (1981).
7. B. A. Dubrovin, A. T. Fomenko, and S. P. Novikov, *Modern Geometry-Methods and Applications, Part I* (Springer-Verlag, New York, 1984).
8. I. S. Gradshteyn and I. M. Ryzhik, *Table of Integrals, Series, and Products* (Academic Press, New York, 1994).
9. A. O. Tsebers, *Magnetohydrodynamics* **16**:236 (1980).
10. J. A. Miranda and M. Widom, *Int. J. Mod. Phys. B* **12**:931 (1998).
11. J. A. Miranda and M. Widom, *Physica D* **120**:315 (1998).